Macromolecules
ARTICLE

Macromolecules **2009**, *42*, 9255–9262 **9255**
DOI: 10.1021/ma901822k

Atom Transfer Radical Polymerization of End-Functionalized Hydrogen-Bonding Polymers and Resulting Polymer Miscibility

Michelle H. Wrue, Aaron C. McUmber, and Mitchell Anthamatten*

Department of Chemical Engineering, University of Rochester, Rochester, New York 14627

Received August 14, 2009; Revised Manuscript Received October 23, 2009

ABSTRACT: The synthesis of end-functionalized hydrogen-bonding polymers and the investigation of their melt phase blend behavior are reported. Monofunctional and telechelic ureidopyrimidinone (UPy)-functionalized poly(styrene)s and poly(methyl methacrylate)s were synthesized using atom transfer radical polymerization (ATRP) followed by atom transfer radical coupling (ATRC). Aggregation of UPy end-groups in solution was observed using size exclusion chromatography. The effect of UPy end-groups on blend miscibility in the melt state was studied using optical microscopy and differential scanning calorimetry. The incorporation of associating groups onto one end of either blend component decreases miscibility relative to unfunctionalized parent blends. Lower miscibility was also observed for blends in which both components were monofunctionalized with associating end-groups. The largest decrease in miscibility was observed for blends containing telechelic UPy-functionalized polymers, which were immiscible across the entire composition range.

Introduction

Polymers containing multiple hydrogen-bonding groups form a rapidly growing subclass of associating polymers that reversibly form aggregates, rings, and chainlike structures.[1−3] Resulting hydrogen-bonded architectures are dynamic and are in equilibrium with their environment—whether in solution or in the melt. Environmental changes in temperature, pH, or solvent can influence hydrogen bond dynamics and alter physical properties. For example, increasing the temperature of associating polymer melts can result in rapid exchange of hydrogen-bonding groups and, consequently, can dramatically lower polymer melt viscosity or elastomer stiffness.[4,5] Such stimuli responsiveness can greatly simplify polymer processing while retaining end-use (typically room temperature) properties and has led to the development of new thermoplastic and healable elastomers[6−12] and shape memory polymers.[13]

Multiple hydrogen-bonding groups may also be useful in engineering miscible polymer blends of traditionally immiscible polymers. Polymer blending provides a straightforward and direct approach to adjusting a material's physical and chemical properties. However, thermodynamic miscibility of polymers is almost always lower than that of small molecules. Polymer−polymer entropy of mixing is usually too low to overcome enthalpic penalties imposed upon mixing. However, hydrogen bonding between polymer blend components can enhance miscibility by overcoming enthalpic differences. There are numerous examples illustrating this approach involving rigid-rod polymers,[14,15] liquid crystals,[16,17] and thermosetting polymer precursors.[18−21] Painter−Coleman's association model has been successfully applied to predict miscibility of several hydrogen-bonding polymer blends.[15,22,23] Key assumptions inherent to this model include random mixing, highly flexible chains, and negligible free volume changes upon mixing.

Despite evidence demonstrating that hydrogen bonding can modify blend behavior, few studies have addressed how site-specific hydrogen-bonding *end-groups* affect melt miscibility. Haruguchi et al. demonstrated that miscibility between poly(styrenes) and poly(ethylene glycols) in solution can be promoted by end-functionalizing components with amine and carboxylate groups, respectively.[24] Their study showed that acid−base reaction of terminal amino groups with carboxylic acid end-groups can promote mixing by inhibiting the formation of terminal carboxylic acid dimers. Multiple hydrogen-bonding end-groups have also been shown to alter melt miscibility,[25,26] resulting, in many cases, in dynamic "pseudo" block copolymers.[26−31] Key features of dynamic block copolymers are (1) simple "mix and match" processing where a library of synthesized homopolymers can be drawn upon to make new materials, (2) faster ordering and inherent reversibility to achieve higher, more robust, long-range order, and (3) tunable nanostructure and properties—since the length scale of phase segregation depends on the homopolymer chain length and the volume fraction of constituent homopolymers. However, synthesis of dynamic block copolymers requires that heterocomplementary binding groups, with high associating constants, can be attached to the ends of homopolymer chains. To this end, controlled radical polymerization techniques have proven especially useful, compared to post-polymerization approaches. Controlled polymerization products have lower polydispersities and are tolerant to a range of functional groups. Moreover, chains can be grown from functionalized initiators, guaranteeing full substitution on chain-ends.

We have previously applied a mean-field model to predict how polymer−polymer miscibility changes if components are functionalized with reversibly binding end-groups.[25] Predicted phase diagrams indicate that self-complementary end-group interactions can stabilize two-phase regions (i.e., promote demixing), giving rise to asymmetric phase diagrams, lower critical solution temperature (LCST)-type behavior, and upper critical solution temperature (UCST)-type behavior. This model broadly agrees with a limited body of experimental data on end-functionalized H-bonding polymer melt blends.[26] Data indicate that self-complementary end-groups slightly encourage compatibilization whereas heterocomplementary groups retard phase separation.

*To whom correspondence should be addressed. E-mail: anthamatten@che.rochester.edu.

Published on Web 11/05/2009

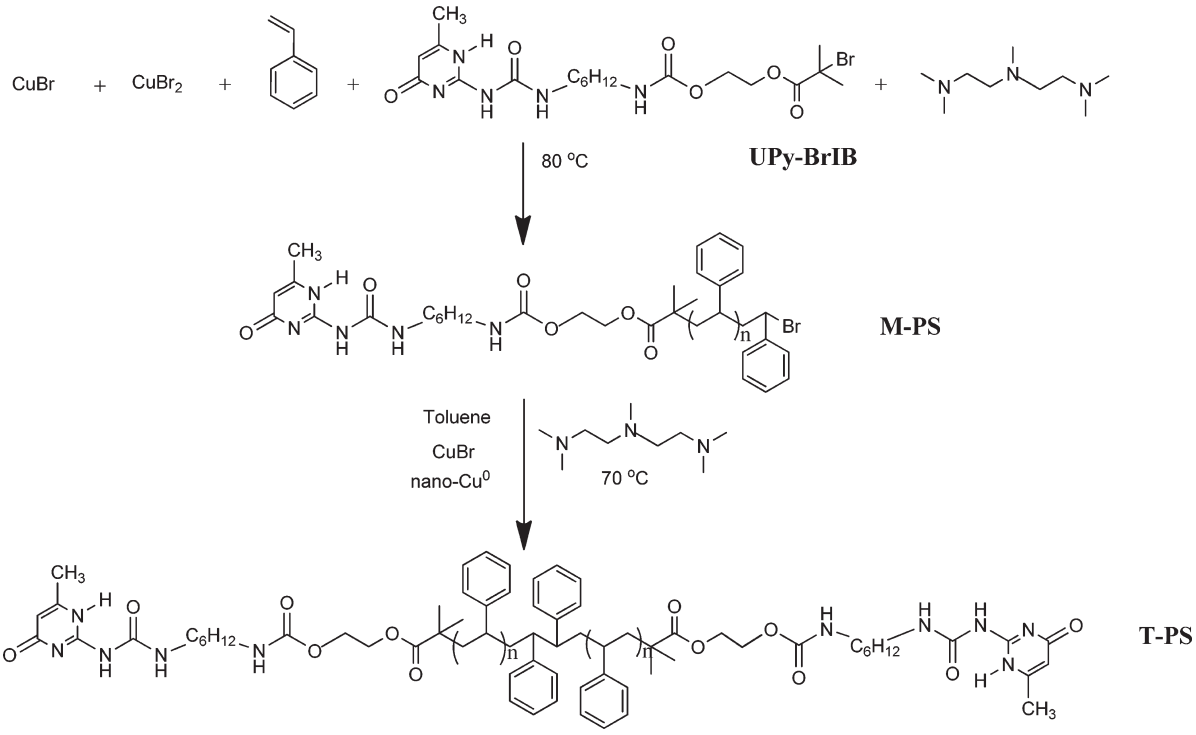

Figure 1. Scheme showing ATRP/ATRC of styrene using a UPy-functionalized bromoisobutyrate initiator to form monofunctional (M-PS) and telechelic (T-PS) polymers.

Here we report an experimental study of how end-association affects polymer−polymer miscibility in the melt. Specifically, we will show how low molecular weight poly(styrene)−poly(methyl methacrylate) (PS/PMMA) miscibility is influenced by both monofunctional and telechelic ureidopyrimidinone (UPy)-terminated polymers. The PS/PMMA blend was chosen because unfunctionalized blends exhibit well-characterized UCST-type phase behavior when at least one component is of low molecular weight (< 4000 g/mol).[32,33] The UPy functional group was chosen because it is a versatile, self-complementary hydrogen-bonding group that has served as a platform for research in associating polymers.[34] The article is organized as follows: first, atom transfer radical polymerization will be described as an effective approach to control molecular weight and ensure all polymer chains are fully substituted with mono- or telechelic UPy end-groups, and next, optical microscopy and calorimetry results from polymer melt miscibility studies will be presented.

Results and Discussion

Synthesis and Characterization of End-Functionalized Polymers. The use of ATRP followed by ATRC to synthesize telechelic polymers has been previously reported.[35−38] For example, Sarbu et al. reported the synthesis of telechelic hydroxy-functionalized polymers by ATRP/ATRC.[36] In the present study study, ATRP/ATRC was used to prepare telechelic UPy-functionalized poly(styrene)s and poly(methyl methacrylate)s. Only low molecular weight PS and PMMA polymers were prepared because the corresponding blends (PS/PMMA) exhibit phase transitions at experimentally accessible temperatures.[33,39,40] To guarantee complete functionalization of all end-groups, a UPy-functionalized, bromoisobutyrate ATRP initiator was synthesized. This was accomplished by first preparing a hydroxy-functionalized ATRP initiator which was subsequently reacted with an isocyanate-terminated UPy synthon[41] to yield a functionalized bromoisobutyrate ATRP initiator (**UPy-BrIB**). The H^1 NMR spectrum of the initiator is available as Supporting Information (Figure S-1).

The reaction scheme showing ATRP/ATRC of styrene from **UPy-BrIB** is illustrated in Figure 1. Copper(I) bromide forms a coordination complex with the amine, *N*,*N*,*N*′,*N*″,*N*″-pentamethyldiethyltriamine (PMDETA), and acts as a catalyst for the polymerization. A small amount of copper(II) bromide is used to control the rate of reaction and limits the concentration of active radicals. A low active polymer radical concentration minimizes the number of growing polymer chains that terminate through radical coupling and disproportionation, affording lower polydispersity. Molecular weight control was achieved by varying the concentration of the initiator and catalyst complex and by varying the reaction time.[42] The monofunctional, bromine-terminated polymer prepared by ATRP then acts as an initiator for the coupling reaction (ATRC). In this second step, a small amount of zerovalent copper metal is used to increase the concentration of radicals, encouraging coupling to form telechelic polymers. The ATRP/ATRC process was repeated using methyl methacrylate as well (scheme not shown).

Following ATRP, proton NMR was used to verify the presence of UPy end-groups (δ = 13.1, 11.9, 10.2 ppm). Functionalization was assumed to be complete because each chain was grown from a functionalized initiator.

Molecular weight characteristics of prepared monofunctional and telechelic polymers are summarized in Table 1. Sample names are chosen to provide the following information: architecture ("M" for monofunctional or "T" for telechelic), backbone type ("PS" or "PMMA"), and molecular weight (in kDa). Compared to ATRP reactions of styrene using 2-hydroxyethyl 2-bromoisobutyrate, the use of UPy-functionalized initiator resulted in similar reaction kinetics, but larger polydispersities (except for **M-PS-6**). However, MMA reaction rates were considerably higher than those reported in the literature. Our ATRP process resulted in PMMA molecular weights at least double those

Table 1. End-Functionalized Associating Polymers Prepared by ATRP/ATRC

sample	M_n (g/mol)[a]	PDI[a]	monomer conversion (%)	coupling efficiency[c]
T-PS-3[b]	12 100	1.95		0.81
M-PS-2	2 300	1.12	17	
T-PS-5	9 700	1.60		0.92
M-PS-6	6 000	1.02	~30	
T-PS-12	48 900	1.49		0.91
M-PS-11	10 700	1.47	38	
T-PS-19	19 000	1.81		0.99
M-PMMA-6	6 300	1.65	17	
T-PMMA-13	19 500	2.32		0.66
M-PMMA-13	13 200	3.01	30	

[a] Determined by GPC. [b] This sample was prepared by UPy functionalization of ATRP prepared HO−PS−OH with M_n = 3060 g/mol and PDI = 1.34. Reported coupling efficiency is for synthesis of HO−PS−OH prior to UPy functionalization. [c] Coupling efficiencies were obtained by nonlinear least-squares fitting of Gaussian peaks to GPC traces, followed by peak integration.

reported by Sarbu et al. under similar conditions with identical reaction times.[36] In addition, the polydispersities for ATRP with MMA were higher than those for styrene. The observed high polydispersities may be due to the increased efficiency of the bulky UPy-functionalized initiator. Increasing the size of the end-group of haloester ATRP initiators has been reported to result in increased efficiency, which can lead to higher polydispersities.[43] A possible approach to improving polydispersities may be to increase the amount of $CuBr_2$ in order to slow the reaction kinetics.

Acquired gel permeation chromatography (GPC) data further indicate that, following ATRC, telechelic polymers exhibit significantly higher molecular weights than their monofunctional precursors. Ideally, ATRC should nearly double the molecular weight. For **T-PS-19** (Figure 2a) this appears to be nearly true—the ATRC reaction increased molecular mass from 10.7 to 19.0 kDa. The corresponding GPC chromatograms are displayed in Figure 2a and provide convincing evidence that the majority of chains were properly coupled. A minor, high molecular weight shoulder is present in this chromatogram. This shoulder also shifted to higher molecular weight following the ATRC reaction. No other samples exhibited this high molecular weight shoulder, and its origin is unknown.

GPC analysis of all other samples following ATRC revealed unexpectedly high molecular weights. In two cases (**T-PS-3** and **T-PS-12**), the chromatograms of coupled polymers showed multiple low retention volume peaks (Figure 2b). For these samples, the resulting average molecular weight of the coupled products was many times that of the monofunctional precursor. The low retention volume elution peaks may be due to self-association of hydrogen-bonding end-groups or possibly to aggregation of UPy end-groups into stacks through hydrogen bonding of the urethane linkage.[34] The resulting aggregates must form structures with time-averaged hydrodynamic radii equivalent to higher molecular weight linear coils. The observation of aggregate formation using chromatography techniques such as GPC and HPLC has been previously reported for Bernard's supramolecular H-bonded star polymers[44] and Gong's H-bonding duplexes.[45] For the UPy-containing polymer studied here, the presence of multiple elution peaks was only observed for lower molecular weight samples. These samples contain a higher weight fraction of UPy end-groups, and this may explain why they are more susceptible to aggregation.[34]

Two experiments were carried out to further investigate the suspected aggregation of **T-PS-12** observed with GPC. A

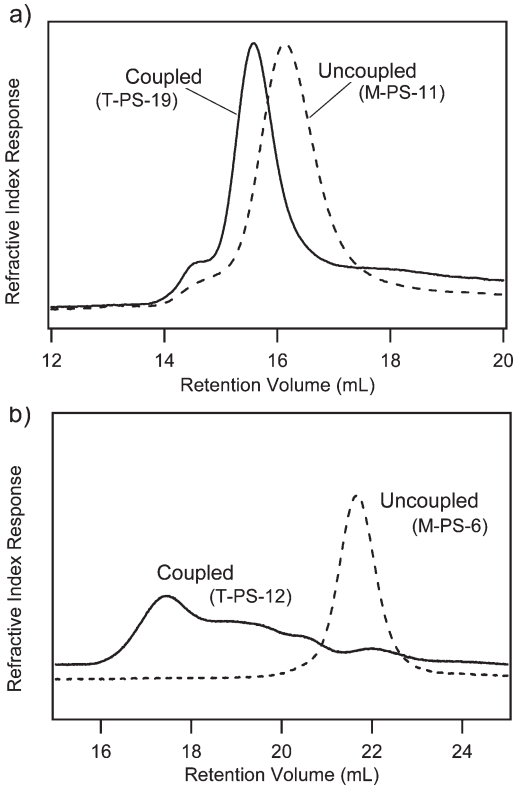

Figure 2. GPC chromatograms of uncoupled and coupled UPy end-functionalized polymers: (a) **M-PS-11** and **T-PS-19**; (b) **M-PS-6** and **T-PS-12**.

small amount of the isocyanate UPy-synthon[41] was added to a solution of **T-PS-12** in THF to intentionally disrupt aggregation. The resulting chromatogram showed a slightly greater amount of free polymer and a lower amount of high molecular weight aggregates compared to the sample without the UPy-synthon (see Figure S-2, Supporting Information). This observation is consistent with earlier studies of UPy-terminated polymers which showed that the addition of "chain stopper" decreases intermolecular association.[4,46] The existence of some aggregation despite the presence of chain stopper indicates that the UPy groups form stable aggregates in solution. In a second experiment, trifluoroacetic acid (TFA) was used to completely remove the associating UPy end-groups by cleavage of urethane or urea functional groups. ^{1}H NMR confirmed that UPy groups were absent while the PS backbone remained intact (see Figure S-3, Supporting Information). The GPC chromatogram for the TFA-washed **T-PS-12** did not show elution peaks that correspond to molecular weights greater than 12 kDa (see Figure S-2, Supporting Information). This confirms that the lower retention volume peaks in Figure 2b are due to end-group aggregation.

Melt Phase Behavior. Films of blended samples were prepared by dissolving polymers into dichloromethane and casting onto glass microscope slides. The average film thickness was measured to be about 30 μm. Cast blends were allowed to dry, and resulting films were vacuum-annealed (150 °C) for 2 h to completely remove solvent and overcome phase separation that may be due to solvent evaporation. The annealing temperature was chosen to be above the glass transition temperature of both blend components. Samples were then slowly cooled (~1 °C/min) to room temperature and were inspected using optical microscopy. Since room temperature is well below the glass transition temperature

(T_g) of both components, this method indicates the phase state at or near the highest T_g of the blend's components. Differential scanning calorimetry was selectively used to corroborate results.

Results will first be presented for two monofunctional blends that showed both mixed and demixed states: PS/M-PMMA and M-PS/PMMA. In both of these blends, one component is UPy-functionalized, and the other component is the "parent" polymer standard. The characteristics of monodisperse standards used in this study are shown in Table 2.

Figure 3 displays typical microscope images for two cast PS/M-PMMA blends. A clear distinction between phase-mixed and phase-separated states was apparent for all blends studied. The length scale of phase separation was about 15 μm, and phase-separated blends generally appeared darker because more light was scattered by the presence of interfaces. Interestingly, phase-separated films were often more brittle than homogeneous films, and cracks were frequently observed. This may be due to the presence of interfaces between the phase-separated domains, along which cracks more easily propagate.

Table 2. Polymer Standards Used in Blend Studies

polymer	M_n (g/mol)	PDI
PS-2	2 400	1.01
PS-4	4 100	1.02
PS-10	10 000	1.03
PS-12	12 500	1.06
PMMA-7	6 700	1.04
PMMA-22	22 200	1.26

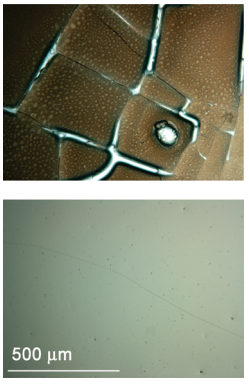

Figure 3. Microscope images of cast blend films of 50/50 **PS-4**/**M-PMMA-6** (top) and 50/50 **PS-2**/**M-PMMA-6** (bottom) showing examples of demixed and mixed states, respectively. The scale bar is the same for both images.

To compare miscibility of end-functionalized polymers with their parent blends, the product of the Flory−Huggins interaction parameter χ and the average degree of polymerization N_{ave} is plotted against volume fraction, ϕ (e.g., Figure 4). Below the critical point, the parent blends should exhibit complete miscibility. Since blends may involve two polymers with different molecular weights, the average degree of polymerization, N_{ave}, is taken to be[47]

$$N_{ave} = \left(\frac{1}{\sqrt{N_A}} + \frac{1}{\sqrt{N_B}}\right)^{-2} \quad (1)$$

The occurrence of the critical point at $\chi N_{ave} = 0.5$ is a consequence of using eq 1 to define the degree of polymerization. Values of χ for parent PS/PMMA blends were calculated from the literature[48] according to $0.028 \pm 3.9/T$ using a temperature of 100 °C, which is close to the T_g of both components. This empirical model of χ was also used when plotting observed miscibility for functionalized polymers. Clearly, this is an approximation since the end-groups occupy a fraction of the backbone and therefore will alter χ. Nevertheless, the approach enables blends containing UPy end-groups to be directly compared to their parent blends.

Figure 4 is a summary of room temperature observations and compares phase behavior of PS/M-PMMA blends to the predicted miscibility of parent (PS/PMMA) blends. This figure displays the observed miscibility of 14 different blends of PS/**M-PMMA-6** following casting, cooling, and annealing. The four different vertical positions correspond to blends prepared using different PS standards (**PS-2**, **PS-4**, **PS-10**, and **PS-12**). **M-PMMA-6** forms homogeneous blends at all compositions when processed with the lowest molecular weight polystyrene (**PS-2**). Figure 4a shows the binodal (solid line) and spinodal (dotted line) stability limits of parent blends containing PS and 6.3 kDa PMMA (the same molecular weight as **M-PMMA-6**). The spinodal line was calculated using the Flory−Huggins equation-of-state model and the stability criterion $\partial^2 \Delta G_m / \partial \phi^2 = 0$, where ΔG_m is change in free energy upon mixing. The binodal line, which indicates the location of the metastable region of the phase diagram, was determined by finding the points of double tangency on a plot of ΔG_m vs ϕ.

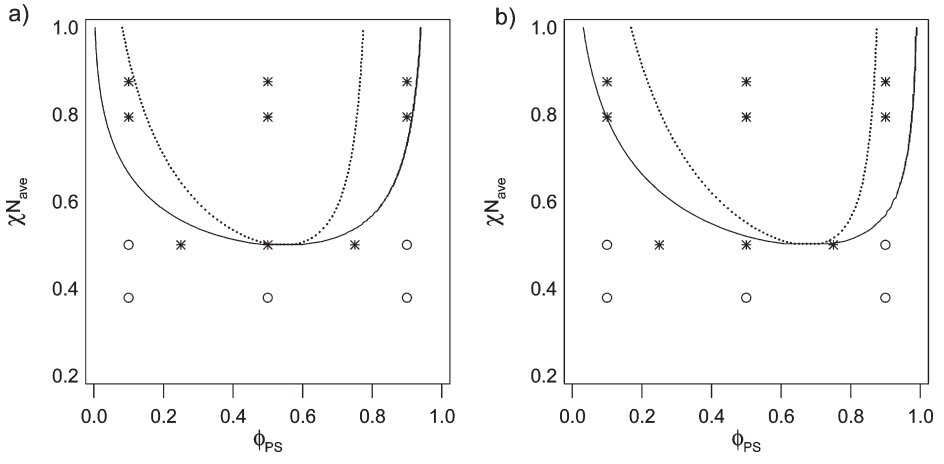

Figure 4. Room temperature observations of miscibility of unfunctionalized polystyrenes of varying molecular weight with **M-PMMA-6**. Open symbols indicate phase-mixed observations. Dashed and solid lines are spinodal and binodal predictions for blends containing (a) 6.3 kDa PMMA and (b) 12.6 kDa PMMA.

Functionalized blends show demixing beneath the parent blend's stability curve, i.e., in the predicted single-phase region. This observation is qualitatively consistent with the prediction that end-group interactions can stabilize two-phase regions.[25] However, it is not clear whether this effect is due to end-to-end association, as predicted. Demixing may also be promoted because of enthalpic differences—the interaction parameter between PS and **M-PMMA-6** may exceed that between PS and PMMA.

To determine whether the observed decrease in miscibility is due to the increased molecular weight upon formation of dimers of **M-PMMA-6**, experimental data are compared with predictions for blends PS and 12.6 kDa PMMA—the same molecular weight as dimers of associated **M-PMMA-6**. Figure 4b shows the binodal (solid line) and spinodal (dotted line) stability limits of parent blends containing this higher molar mass PMMA. Again, the functionalized blends show demixing within the predicted single-phase region. Therefore, the decreased miscibility cannot be attributed to increase in molecular weight alone (upon association to form dimers). The stabilization of the two-phase region of the phase diagram is likely due to a combination of end-to-end association, the formation of stacks by hydrogen bonding of the adjacent urethane linkages, and enthalpic differences between UPy end-groups and homopolymers.

While optical microscopy offers easy sample preparation and small sample sizes, it can be limited by the size of the phase-separated domains. Using this technique, if phase-separated domain sizes are too small to be imaged, samples may falsely appear to be homogeneous even though phase separation has occurred. In light of this concern, DSC experiments were used to corroborate optical microscopy results. DSC is frequently used to evaluate blend miscibility.[49−51] The presence of a single glass transition temperature T_g, intermediate to the T_gs of pure components, indicates blend miscibility. The appearance of two T_gs is evidence of two distinct phases of differing composition. DSC data were collected for blends of **PS-4** with **M-PMMA-6** as well as for the pure materials. Results are shown in Figure 5. In good agreement with optical microscopy data in Figure 4, single T_gs were observed for the 90/10 and 10/90 blends, and two separate T_gs were observed for the 49/51 blend. Note that the T_g of the UPy-functionalized PMMA is significantly higher than that of its parent. This observation, that UPy-functionalization increases T_g, is consistent with reports by several others.[34,52,53] The Supporting Information (Figure S-4) provides DSC scans which provide more evidence regarding this effect.

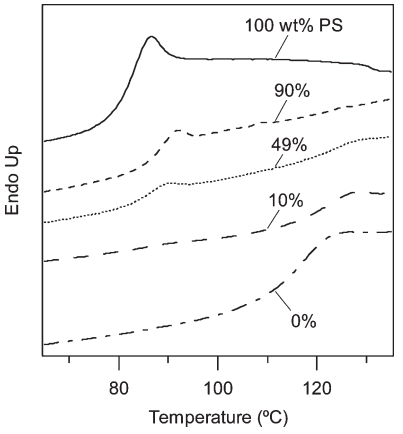

Figure 5. DSC second heating thermograms for **PS-4**, **M-PMMA-6**, and their blends.

Ten blends were also prepared in which monofunctional polystyrene (**M-PS-2**) was mixed with various PMMA standards. Optical microscopy results are shown in Figure 6. The two different vertical positions correspond to blends prepared using **PMMA-7** and **PMMA-22**. Figure 6a shows the binodal (solid line) and spinodal (dotted line) stability limits of parent blends containing PMMA and 2.4 kDa PS (the same molecular weight as **M-PS-2**). Figure 6b shows the binodal (solid line) and spinodal (dotted line) stability limits of parent blends containing containing PMMA and 4.8 kDa PS (the same molecular weight as dimers of associated **M-PS-2**). As described in the discussion of Figure 4, these lines were calculated using the Flory−Huggins equation-of-state model and the stability criterion. **M-PS-2** formed homogeneous blends at all compositions except the 50/50 blends when processed with either weight poly(methyl methacrylate) standard. Experimental observations of miscibility differ significantly from predictions based on unimers of **M-PS-2** (Figure 6a) as well as predictions based on dimers of **M-PS-2** (Figure 6b). A slightly better agreement is observed when molecular weight of dimers is considered.

The miscibility of blends in which both components were monofunctional was also investigated. Optical microscopy results are shown in Figure 7 which again delineates predicted binodal (solid line) and spinodal (dotted line) stability limits of parent blends containing PS and 13 kDa PMMA (the same molecular weight as **M-PMMA-13**). As indicated by the observation of phase separation within the predicted

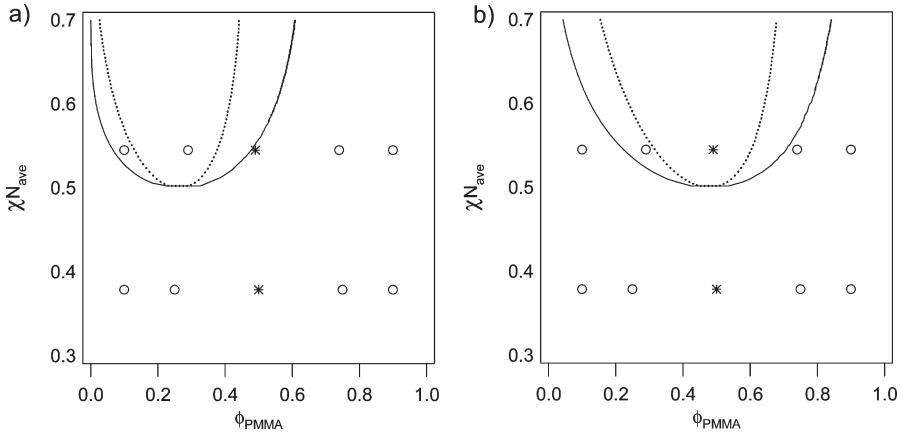

Figure 6. Room temperature observations of miscibility of **PMMA-7** and **PMMA-27** with **M-PS-2**. Open symbols indicate phase-mixed observations. Dashed and solid lines are spinodal and binodal predictions for blends containing (a) 2.4 kDa PS and (b) 4.8 kDa PS.

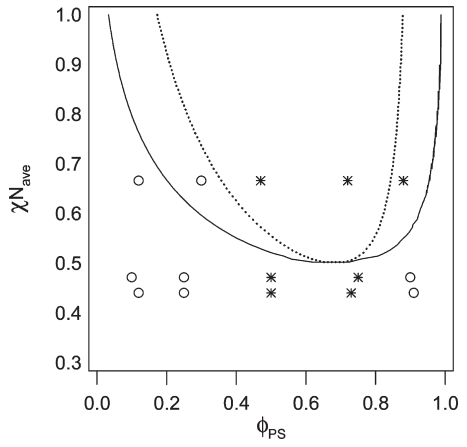

Figure 7. Room temperature observations of miscibility of M-PSs with M-PMMAs of varying molecular weights. Open symbols indicate phase-mixed observations. Dashed and solid lines are spinodal and binodal predictions for blends of PS with 13 kDa PMMA.

single phase region, there is a reduction in miscibility observed for these blends that offer the possibility of interassociation, as well as self-association. Additionally, experimental observations display asymmetry in the phase diagram that is qualitatively captured by the predictions.

Telechelic materials prepared by ATRC were also used in blend studies. All blends containing telechelic materials were immiscible. For example, blends of **T-PS-9** with **T-PMMA-13** were immiscible across the entire composition range. We attribute this either to end-to-end association of telechelic polymers to form longer chains or to the stacking of UPy end-groups.[34] Considering our GPC observations discussed in the prior section, low molar mass telechelic polymers are more prone to forming aggregates, even in solution. These aggregates are remarkably stable and are able to pass through elevated-temperature (60 °C) chromatography columns. Given this observation of aggregates in solution, aggregates are likely present at the time of casting, which would kinetically hinder the formation of a single mixed phase upon annealing. Nevertheless, end-to-end association or stacking of end-groups should result in blend components with greater effective molecular weights, partly explaining the observed in decrease miscibility.

Feldman et al. previously reported miscibility of low-T_g (meth)acrylic polymers containing monofunctional UPy and 2,7-diamido-1,8-naphthyridine (Napy) end-groups.[26] Their study showed that the phase behavior is largely influenced by end-group specificity. Blends with each component containing a self-complementary UPy end-group showed slight compatibilization, whereas blends containing UPy−Napy (heterocomplementary) groups lead to significant retardation of phase separation. In the present study, two high-T_g polymers were considered (PMMA and PS) containing self-complementary UPy end-groups. The observed miscibility is indicative of the phase state near the highest T_g—typically ~100 °C. However, the equilibrium degree of association near 100 °C may be significantly lower than that occurring near room temperature, and this may limit the ability of hydrogen-bonding end-groups to compatibilize the blend. Furthermore, kinetic issues may be important. On the one hand, around 100 °C, UPy groups have much higher dissociation rates than at room temperature, and this should promote more rapid equilibration of phase state. On the other hand, unlike the Feldman study, the self-complementary end-groups are connected to the polymer backbone using urethane linkages that, in addition to end-to-end association, are capable of intermolecular stacking.[34] The present study highlights that decreased miscibility is not due to end-to-end association alone. Enthalpic differences between end-groups and backbones as well as end-group aggregation may play equally important roles.

Conclusions

ATRP/ATRC using a functionalized initiator was successfully carried out to prepare ureidopyrimidinone-functionalized monofunctional and telechelic PS and PMMA samples of various low molecular weights. While styrene reaction rates were similar to other published results, methyl methacrylate polymerization rates were greater than reported. Higher polymerization rates and rather high polydispersities were attributed to increased efficiency of the UPy-functionalized initiator. Solution aggregation of UPy end-groups was observed using size-exclusion chromatography for low molecular weight telechelic polymers and is attributed to association of UPy end-groups or the formation of end-group stacks via the urethane linkages. Experiments using a "chain stopper" to interfere with the formation of long chains of associated telechelic polymers only slightly changed the population distribution of aggregates, indicating that solution aggregates have a high stability.

The incorporation of UPy groups onto any or all components of the PS/PMMA blends lowered polymer−polymer miscibility. The observed stabilization of the two-phase region of the phase diagram is likely due to a combination of end-to-end association, the formation of stacks by hydrogen bonding of adjacent urethane linkages, and enthalpic differences between UPy end-groups and homopolymers. The greatest effect was observed for blends of two telechelic materials, which were immiscible across the entire composition range. End-group aggregation or stacking in synthesized telechelic samples likely has a large effect on the kinetics of mixing. It is probable that aggregates were present in our solutions prior to casting films, which could impede the formation of phase-mixed blends.

Experimental Section

Materials. *Functionalized Initiator Synthesis.* 2-Amino-4-hydroxy-6-methylpyrimidine (2-AHMP, Alfa Aesar), 1,6-hexane diisocyanate (HDI), pentane (EMD), pyridine (Sigma-Aldrich), dibutyltin dilaurate (DBTDL, Alfa Aesar), ethylene glycol (Aldrich), *N,N*-dicylcohexylcarbodiimide (DCC, Aldrich), 2-bromo-2-methylpropionic acid (BMP, Sigma-Aldrich), dichloromethane (DCM, Aldrich), and (dimethylamino)pyridine (DMAP, Aldrich).

Functionalized Polymer Synthesis (*ATRP*/*ATRC*). Styrene (Sigma), methyl methacrylate (MMA, Alfa Aesar), copper(I) bromide (CuBr, Sigma-Aldrich), copper(II) bromide ($CuBr_2$, Sigma-Aldrich), *N*,*N*,*N*′,*N*′,*N*″-pentamethyldiethylenetriamine (PMDETA, Aldrich), nanocopper (Aldrich), acetone (Mallinckrodt), and toluene (Mallinckrodt).

Purification of Materials. CuBr was washed with glacial acetic acid, followed by isopropanol. The washed CuBr, $CuBr_2$, and UPy-functionalized initiator were dried at 60 °C in a vacuum oven overnight immediately before use. 1,6-Hexane diisocyanate, styrene, methyl methacrylate, and PMDETA were each distilled before use. All liquid reagents used in ATRP/ATRC procedures were bubbled with nitrogen gas for at least 30 min immediately before use. All other materials were used as received.

Synthesis. *2-Hydroxyethyl 2-Bromoisobutyrate* (*HEBriBu*) *Catalyst*. 200 mL of anhydrous dichloromethane was added to a reaction flask with 18.7 g of ethylene glycol, 32.5 g of DCC, and 26.3 g of BMP. The flask was cooled in an ice−water bath, and 197 mg of DMAP was added. After cooling for 15 min, the flask was removed from the bath, allowed to warm to room

temperature, and stirred overnight. The reaction mixture was filtered to remove precipitated dicylcohexylurea. Crude product was recovered by evaporation of solvent from the filtrate. The product was purified using gradient column chromatography with 4/1 to 2/3 hexane/diethyl ether as the mobile phase. Product is pale yellow liquid, 5.63 g after purification (15% yield). The product was confirmed by ^{1}H NMR (400 mHz, $CDCl_3$): δ = 4.31(t, 2H, J_{HH} = 3.2 Hz, OCH_2CH_2OH), 3.86 (t, 2H, J_{HH} = 4.0 Hz, OCH_2CH_2OH), 1.95 (s, 6H, $C(Br)CH_3$).

2-(6-Isocyanatohexylaminocarbonylamine)-6-methyl-4-[1H]-pyrimidinone (UPy-NCO). To a 250 mL dried reaction flask 17.5 g of 2-AHMP, 12.0 mL of pyridine, and 154 mL of HDI were added. The flask was stirred in a 110 °C oil bath for 18 h. The flask was removed from the bath and cooled to room temperature, and pentane was added to precipitate product. The filtered product, a white solid, was dried in a 50 °C vacuum oven overnight. Final yield = 39.2 g (96% yield). Formation of the product was confirmed by ^{1}H NMR (400 mHz, $CDCl_3$): δ = 13.1 (s, 1H, CH_3CNH), 11.9 (s, 1H, $CH_2NH(C{=}O)NH$), 10.2 (s, 1H, $CH_2NH(C{=}O)NH$), 5.8 (s, 1H, $CH{=}CCH_3$), 3.2 (m, 4H, $NH(C{=}O)NHCH_2 + CH_2NCO$), 2.2 (s, 3H $CH_3C{=}CH$), 1.6 (m, 4H, NCH_2CH_2), 1.4 (m, 4H, $CH_2CH_2CH_2CH_2CH_2$).

UPy-Functionalized Initiator (UPy-BrIB). 250 mL of dried chloroform (dried over molecular sieves), 1.60 g of HOEBriBu, 6.51 g of UPy-NCO, and 2 drops of DBTDL were added to a 500 mL round-bottom flask with a stir bar and a condenser. The flask was immersed in a 65 °C oil bath and stirred for 16 h. An additional 200 mL of $CHCl_3$ was added, and the mixture was filtered. The filtrate volume was reduced to 250 mL under vacuum, 2.55 g of silica gel and 1 drop of DBTDL were added, and the reaction was allowed to proceed for an additional hour at 65 °C. The silica gel was removed by filtration, and the solvent was removed under vacuum. The resulting white powder was dried completely in 50 °C vacuum oven overnight. Final yield was 3.67 g (99% yield). ^{1}H NMR was used to confirm attachment of UPy groups (see Figure S-3, Supporting Information) (400 mHz, $CDCl_3$): δ = 13.1 (s, 1H, CH_3CNH), 11.9 (s, 1H, $CH_2NH(C{=}O)NH$), 10.2 (s, 1H, $CH_2NH(C{=}O)NH$), 5.8 (s, 1H, $CH{=}CCH_3$) 4.31 (m, 4H, $CH_2CH_2OC(=O)NH + CH_2CH_2OC(=O)$), 3.2 (m, 4H, $NH(C{=}O)NHCH_2 + CH_2NCO$), 2.2 (s, 3H, $CH_3C{=}CH$), 1.95 (s, 6H, $C(Br)CH_3$), 1.6 (m, 4H, NCH_2CH_2), 1.4 (m, 4H, $CH_2CH_2CH_2CH_2CH_2$).

UPy-Functionalized Poly(methyl methacrylate) (M-PMMA) and Polystyrene (M-PS). In a typical experiment, 126 mg of copper(I) bromide, 41.5 mg of copper(II) bromide, 524 mg of UPy-BrIB initiator, and a stir bar were added to a dried 100 mL Schlenk flask. The flask was degassed and backfilled with N_2 three times. Methyl methacrylate (7.90 mL) and 5.00 mL of acetone were added, and three freeze−dry−thaw cycles were performed. PMDETA (0.20 mL) was added by dried syringe, and the solution was stirred until color change indicated the complex had formed. The flask was immersed in a 55 °C oil bath for 1 h. The reaction was then stopped by exposure to air and diluted with tetrahydrofuran (THF). Residual copper was removed by passing through an alumina column. The product was then precipitated in methanol. After filtration, the white solid product was dried in a 60 °C vacuum oven overnight. Yield = 1.37 g. Product was characterized by GPC to give, e.g., M_n = 6300 g/mol and PDI = 1.65.

A similar procedure was used for polymerization of styrene at 80 °C. Acetone was not used for styrene synthesis. Alteration of the molar ratios of the reactants, along with reaction time, was used to prepare samples of differing molecular weights.

T-PS and T-PMMA. For the coupling of 6300 g/mol UPy-PMMA-Br, 15.9 mg of copper(I) bromide, 26.9 mg of nanocopper powder, 701 mg of UPy-PMMA-Br, and a stir bar were added to a dried 100 mL Schlenk flask. The flask was degassed and backfilled with N_2 three times. 10.0 mL of toluene was added and stirred to dissolve the polymer. Three freeze−dry−thaw cycles were performed, and PMDETA (0.05 mL) was added by dried syringe. The reaction was carried out in 80 °C oil bath overnight. The reaction was stopped by exposure to air and diluted with tetrahydrofuran (THF). Residual copper was removed by passing through an alumina column. The product was precipitated into an 80/20 methanol/water mixture. After filtration, the white solid product was dried in a 60 °C vacuum oven overnight. Product was characterized by GPC to give M_n = 19 500 g/mol and PDI = 2.32. The same procedure was used for coupling of UPy-PS-Br samples.

Structure Characterization. Structure determinations were carried out in deuterated chloroform using a Bruker Avance 400 MHz NMR spectrometer. The molecular weights of prepared polymers were measured by gel permeation chromatography (GPC). GPC instrumentation consisted of an Agilent 1100 HPLC system equipped with a Viscotek triple detector. Three columns were utilized (two Viscotek mixed bed, low M_w, i-series and one mixed bed medium M_w, i-series column). The system temperature was maintained at 60 °C for NMP eluent and 30 °C for THF eluent. Calibration was performed using various molecular weight polystyrene standards. GPC traces were interpreted using the instrument software package Omni-SEC (Viscotek).

Blend Characterization. Optical microscopy experiments were performed using a Leica DML optical microscope. Digital images were acquired using a Leica DFC 320 CCD camera. DSC experiments were performed on a Perkin-Elmer DSC 7 with Perkin-Elmer Pyris Thermal Analysis Software, v. 6.0.0.0033. Scans were performed from −30 to 180 °C at a heating/cooling rate of 20 °C/min, and only second heating scans are reported.

Acknowledgment. Acknowledgment is made to the donors of The American Chemical Society Petroleum Research Fund for support of this research and the National Science Foundation under DMR-0906627. M. H. Wrue acknowledges support from a Horton Fellowship administered through the Laboratory of Laser Energetics.

Supporting Information Available: Additional ^{1}H NMR spectra and GPC chromatograms. This material is available free of charge via the Internet at http://pubs.acs.org.

References and Notes

(1) Wilson, A. J. *Soft Matter* **2007**, *3*, 409–425.
(2) Farnik, D.; Kluger, C.; Kunz, M. J.; Machl, D.; Petraru, L.; Binder, W. H. *Macromol. Symp.* **2004**, *217*, 247–266.
(3) Bouteiller, L. *Adv. Polym. Sci.* **2007**, *207*, 247–266.
(4) Sijbesma, R. P.; Beijer, F. H.; Brunsveld, L.; Folmer, B. J. B.; Hirschberg, J. H. K. K.; Lange, R. F. M.; Lowe, J. K. L.; Meijer, E. W. *Science* **1997**, *278* (5343), 1601–1604.
(5) Hirschberg, J. H. K. K.; Beijer, F. H.; van Aert, H., A.; Magusin, P. C. M. M.; Sijbesma, R. P.; Meijer, E. W. *Macromolecules* **1999**, *32* (8), 2696–2705.
(6) Yamauchi, K.; Lizotte, J. R.; Long, T. E. *Macromolecules* **2003**, *36* (4), 1083–1088.
(7) Lange, R. F. M.; Van Gurp, M.; Meijer, E. W. *J. Polym. Sci., Part A: Polym. Chem.* **1999**, *37* (19), 3657–3670.
(8) Sivakova, S.; Bohnsack, D. A.; Mackay, M. E.; Suwanmala, P.; Rowan, S. J. *J. Am. Chem. Soc.* **2005**, *127* (51), 18202–18211.
(9) Botterhuis, N. E.; van Beek, D. J. M.; van Gemert, G. M. L.; Bosman, A. W.; Sijbesma, R. P. *J. Polym. Sci., Part A: Polym. Chem.* **2008**, *46* (12), 3877–3885.
(10) Cordier, P.; Tournilhac, F.; Soulie-Ziakovic, C.; Liebler, L. *Nature* **2008**, *451*, 977–980.
(11) Nair, K. P.; Breedveld, V.; Weck, M. *Macromolecules* **2008**, *41* (10), 3429–3438.
(12) Kautz, H.; van Beek, D. J. M.; Sijbesma, R. P.; Meijer, E. W. *Macromolecules* **2006**, *39* (13), 4265–4267.
(13) Li, J.; Viveros, J. A.; Wrue, M. H.; Anthamatten, M. *Adv. Mater.* **2007**, *19*, 2851–2855.
(14) Cowie, J. M. G.; Nakata, S.; Adams, G. W. *Macromol. Symp.* **1996**, *112*, 207–216.

(15) Painter, P. C.; Tang, W. L.; Graf, J. F.; Thomson, B.; Coleman, M. M. *Macromolecules* **1991**, *24* (13), 3929–3936.
(16) Kato, T.; Frechet, J. M. J. *Macromol. Symp.* **1995**, *98*, 311–316.
(17) Viswanathan, S.; Dadmun, M. D. *Macromolecules* **2003**, *23* (9), 3196–3205.
(18) Zheng, H. F.; Zheng, S. X.; Guo, Q. P. *J. Polym. Sci., Part A: Polym. Chem.* **1997**, *35* (15), 3169–3179.
(19) Lu, H.; Zheng, S. *Polymer* **2003**, *44*, 4689–4698.
(20) Ni, Y.; Zheng, S. X. *Polymer* **2005**, *46* (15), 5828–5839.
(21) Kim, S.; Kim, H. J. *Macromol. Mater. Eng.* **2007**, *292* (3), 339–346.
(22) Coleman, M. M.; Painter, P., C. *Prog. Polym. Sci.* **1995**, *20*, 1–59.
(23) Painter, P. C.; Park, Y.; Coleman, M. M. *Macromolecules* **1989**, *22* (2), 580–585.
(24) Haraguchi, M.; Nakagawa, T.; Nose, T. *Polymer* **1995**, *36* (13), 2567–2572.
(25) Anthamatten, M. *J. Polym. Sci., Part B: Polym. Phys.* **2007**, *45*, 3285–3299.
(26) Feldman, K. E.; Kade, M. J.; de Greef, T. F. A.; Meijer, E. W.; Kramer, E. J.; Hawker, C. J. *Macromolecules* **2008**, *41* (13), 4694–4700.
(27) Fleischer, C. A.; Morales, A. R.; Koberstein, J. T. *Macromolecules* **1994**, *27* (2), 379–385.
(28) Noro, A.; Nagata, Y.; Takano, A.; Matsushita, Y. *Biomacromolecules* **2006**, *7* (6), 1696–1699.
(29) Binder, W. H.; Kunz, M. J.; Ingolic, E. *J. Polym. Sci., Part A: Polym. Chem.* **2004**, *42*, 162–172.
(30) Park, T.; Zimmerman, S. C. *J. Am. Chem. Soc.* **2006**, *128*, 13986–13987.
(31) Huh, J.; Park, H. J.; Kim, K. H.; Kim, K. H.; Park, C.; Jo, W. H. *Adv. Mater.* **2006**, *18*, 624–629.
(32) Fekete, E.; Foldes, E.; Pukansky, B. *Eur. Polym. J.* **2005**, *41*, 727–736.
(33) Massa, D. J. Physical Properties of Blends of Polystyrene with Poly(methyl Methacrylate) and Styrene/(methyl Methacrylate) Copolymers. In *Multiphase Polymers*; ACS Advances in Chemistry Series; Cooper, S. L., Estes, G. M., Eds.; American Chemical Society: Anaheim, CA, 1979; Vol. *176*, pp 433−442.
(34) van Beek, D. J. M.; Spiering, A. J. H.; Peters, G., W. M.; Nijenhuis, K. t.; Sijbesma, R. P. *Macromolecules* **2007**, *40*, 8464–8475.
(35) Yurteri, S.; Cianga, I.; Yagci, Y. *Macromol. Chem. Phys.* **2003**, *204* (14), 1771–1783.
(36) Sarbu, T.; Lin, K.-Y.; Spanswick, J.; Gil, R. R.; Siegwart, D. J.; Matyjaszewski, K. *Macromolecules* **2004**, *37* (26), 9694–9700.
(37) Kopping, J. T.; Tolstyka, Z. P.; Maynard, H. D. *Macromolecules* **2007**, *40* (24), 8593–8599.
(38) Toquer, G.; Monge, S.; Antonova, K.; Blanc, C.; Nobili, M.; Robin, J. J. *Macromol. Chem. Phys.* **2007**, *208* (1), 94–102.
(39) Ougizawa, T.; Walsh, D. J. *Polym. J.* **1993**, *25* (12), 1315–1318.
(40) Buki, L.; Gonczy, E.; Fekete, E.; Hellman, G. P.; Pukansky, B. *Macromol. Symp.* **2001**, *170*, 9–20.
(41) Folmer, B. J. B.; Sijbesma, R. P.; Versteegen, R. M.; van der Rijt, J. A. J.; Meijer, E. W. *Adv. Mater.* **2000**, *12* (12), 874–878.
(42) Sarbu, T.; Lin, K.-Y.; Ell, J.; Siegwart, D. J.; Spanswick, J.; Matyjaszewski, K. *Macromolecules* **2004**, *37* (9), 3120–3127.
(43) Matyjaszewski, K.; Xia, J. *Chem. Rev.* **2001**, *101* (9), 2921–2990.
(44) Bernard, J.; Lortie, F.; Fenet, B. *Macromol. Rapid Commun.* **2009**, *30* (2), 83–88.
(45) Li, M.; Yamato, K.; Ferguson, J. S.; Gong, B. *J. Am. Chem. Soc.* **2006**, *128*, 12628–12629.
(46) Keizer, H. M.; van Kessel, R.; Sijbesma, R. P.; Meijer, E. W. *Polymer* **2003**, *44* (19), 5505–5511.
(47) Robeson, L. M. *Polymer Blends: A Comprehensive Review*; Hanser Gardner Publications, Inc.: Cincinnati, OH, 2007.
(48) Russell, T. P.; Hjelm, R. P.; Seeger, P. A. *Macromolecules* **1990**, *23*, 890–893.
(49) Dreezen, G.; Groeninckx, G.; Swier, S.; Van Mele, B. *Polymer* **2001**, *42*, 1449–1459.
(50) Lu, H.; Zheng, S.; Tian, G. *Polymer* **2004**, *45*, 2897–2909.
(51) Tang, M.; Liau, W.-R. *Eur. Polym. J.* **2000**, *36*, 2597–2603.
(52) Tang, L. M.; Wang, Y.; Qiu, Y. P.; Guan, S. Y. *Acta Polym. Sin.* **2009**, *1*, 93–96.
(53) Cao, Y.; Wang, Y.; Li, B. T.; Tang, L. M. *Chin. J. Polym. Sci.* **2008**, *26* (6), 767–774.